IEEE Transactions on Nuclear Science, Vol. NS-29, No. 6, December 1982

# COLLECTION OF CHARGE ON JUNCTION NODES FROM ION TRACKS

G. C. Messenger*

Rockwell International
Autonetics Strategic Systems Division
Defense Electronics Operations
3370 Miraloma Avenue
Anaheim, CA 92803

## Abstract

The collection of charge from ion tracks can produce logic upset and memory change in high density integrated circuits. It has been experimentally observed that drift conduction usually plays a dominant role when the ion track penetrates a junction.[1] The first charge collection analysis concentrated on the diffusion conduction process.[2] A recent analysis emphasizes drift conduction and describes the "funnel" which produces drift collection from the substrate.[3] The funneling phenomenon has been modelled using two-dimensional computer simulations.[4] It is extremely desirable to develop analytical solutions tp better understand the problem and to provide the basis for modelling the effect in circuit and system analysis computer codes such as SYSCAP. This paper develops an approximate analytic solution expressed as

$$I(t) = I_o [\exp(-\alpha t) - \exp(-\beta t)] \quad (1)$$

where $I_o$ is approximately the maximum current, $1/\alpha$ is the collection time constant of the junction, and $1/\beta$ is the time constant for initially establishing the ion track. The junction time constant is shown to be $K\epsilon_o/q\mu N_D$, and it increases slowly with funnel length when a funnel is present. The analysis shows that the excess carriers move almost exclusively by ambipolar diffusion for very early times, and that the fields present in semiconductor devices, including p-n junction fields, collapse. Ambipolar diffusion proceeds until the excess carrier concentration is reduced to approximately the background doping density at which time the junction field is restored and the carriers move by drift. The funnel is produced by the IR drop in the substrate as a consequence of the high current density produced by collecting the excess charge in the ion track. The applied voltage, $V_A$, then redistributes so that

$$V_A = V_J + I_o R_S \quad (2)$$

where $R_S$ is the substrate spreading resistance. The funnel length is then approximately the junction width multiplied by $I_o R_S/V_J$ since the field is approximately linear.

## First Order Theory

The basic processes are governed by the continuity equations for the hole electron pairs in the ion track. The basic geometry is shown in Figure 1, and the basic response in Figure 2.

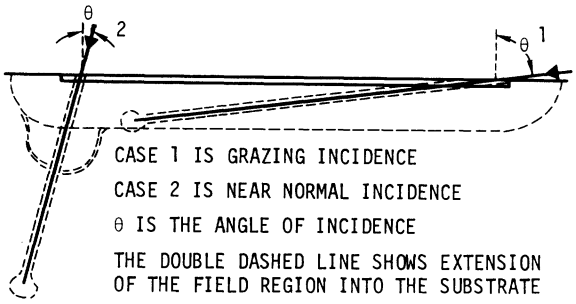


Figure 1. Ion Tracks Through a P+N Junction

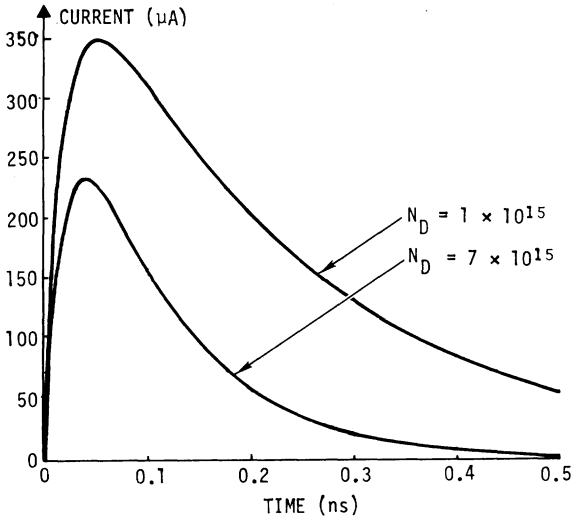


Figure 2. Transient Response for a 5 MeV α Particle Calculated as Described in the Discussion of Funnel Phenomenon

The governing equation set is

$$\begin{aligned} \frac{dp}{dt} &= Gp - Up - 1/q\ \nabla \cdot Jp \\ Jp &= q\mu_p pE - qDp\nabla p \\ \frac{dn}{dt} &= Gn - Un + 1/q\ \nabla \cdot Jn \\ Jn &= q\mu_n nE + qDn\nabla n \end{aligned} \quad (3)$$

In addition, Poisson's equation is required:

$$\nabla^2 V = -\rho/k\epsilon_o \quad (4)$$

*Consultant to Rockwell International

Some of this work was performed under Contract No. F04704-78-C-0021.



0018-9499/82/1200-2024$00.75©1982 IEEE

Assume a cylindrical track of hole electron pairs with an initial radius less than approximately $0.1\mu$[5]. The generation rate along the track is a slowly varying function and is approximately $4 \times 10^8$ hep/cm for a 5 MeV α-particle. Assume that the generation rate is constant along the path. This reduces the problem to cylindrical geometry and is a very good approximation since the concentration gradients along the track are orders of magnitude smaller than the concentration gradient in the radial direction. The time required to create the initial charge density along the track is less than 10 picoseconds. The value of β in eq (1) is assumed to be $>10^{11}$ $s^{-1}$; this assumption has a negligible effect on subsequent transient calculations. The initial charge density in the ion track will exceed $10^{18}/cm^3$. This is much greater than the doping density or majority carrier density in the substrate and therefore subsequent motion of these carriers must be ambipolar.

Ion Tracks in Homogeneous Bulk Silicon

First consider an ion track created in homogeneous bulk silicon and neglect any end effects. Let the Linear Energy Transfer (LET) be a slowly varying quantity along the track so that the problem becomes exactly cylindrical. The boundary conditions in eq (3) after the track has formed become

$$Gp = Gn = N = LET/3.6\ eV \qquad (5)$$

LET may now be related to a specific ion or to the Heinrich curves for the cosmic ray environment in space.[6] Typical values of N range from $10^7$ hole electron pairs (hep)/cm to $10^{11}$ hep/cm. Initial carrier concentrations exceed the background doping concentrations for silicon regions of interest and require reduction of eq (3) to ambipolar form. This is done by assuming charge neutrality and leads to

$$D^*\nabla^2\delta p - \mu^* E \cdot \nabla\delta p - \frac{\delta p}{\tau} = \frac{\partial \delta}{\partial t} \qquad (6)$$

with a similar equation for δn.

At long times, carrier motion is governed by the ordinary continuity equation which has exactly the same form with D* and μ* replaced by $D_p$ and $\mu_p$. The generation function is assumed radially symmetric,[5] that is, $\delta p(r,o) = NF(r)$. Jaffe[7] assumed $\delta p = N/\pi b^2 \exp(-r^2/b^2)$ where b was an assumed value of radius at t = 0. It is noted that the assumption of radial symmetry may not always be exactly correct. For example, statistical variations such as collision with a nucleus or creation of δ rays might produce variations from radial symmetry.[9] The lifetime, τ, is assumed constant. This assumption is probably incorrect. However, the relaxation of carrier concentrations to levels wnere τ is constant occurs so rapidly in silicon that the reduced lifetime at ve00 early times will not produce a consequential error. The diffusion constant will vary from D* at early times to $D_p$ at long times. This variation is removed from the integration, since it is a relatively weak function of concentration, and inserted in the solution as a transition function. This follows a technique originally used by Jaffe,[7] and makes it possible to obtain a good approximate solution in closed form. First let E = 0. The general solution to eq (6) is then,

$$\delta p(r,t) = \frac{N}{2D^*t} \exp(-r^2/4D^*t - t/\tau) \int_0^\infty uF(u)\exp(-u^2/4D^*t) I_o\left(\frac{ur}{2D^*t}\right) du \qquad (7)$$

A specific solution to eq (6) with F(u) replaced by a two-dimensional Dirac delta function is given by

$$\delta p(r,t) = \frac{N}{4\pi Dt} \exp(-r^2/4Dt - t/\tau) \qquad (8)$$

where

$$D = \frac{(n_i+2\delta p)DpDn}{(n_i+\delta p)Dn+\delta pDp}\ , \text{ see Appendix A.}$$

Here $n_i \simeq N_D$, the doping concentration in the silicon material.

Now a solution to eq (6) can be obtained with a constant field $E_C$ in the X direction and a generation function N.

$$\delta p(x,y,t) = \frac{N}{4\pi Dt} \exp\left(-\frac{(x-\mu E_C t)^2+y^2}{4Dt} - \frac{t}{\tau}\right) \qquad (9)$$

where

$$\mu = \frac{n_i\ \mu_n\ \mu_p}{(n_i+\delta p)\ \mu_n+\delta p\mu_p}\ , \quad \text{see Appendix A.}$$

The solution along the X-axis is compared to eq (8) and eq (9) in Figure 3. The effect of the field is to move the distribution along the X-axis a distance of $\mu E_C t$.

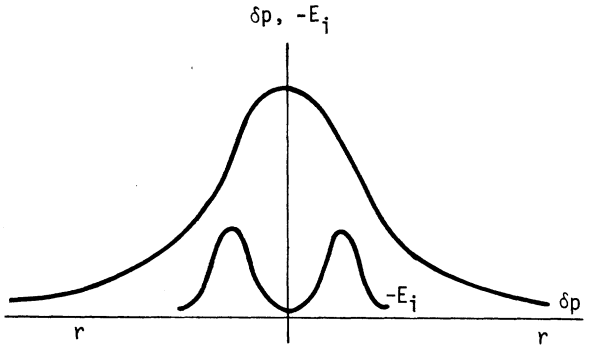


Figure 3. Carrier Concentration and Radial Field for Cylindrical Geometry

The basic approximation used to derive the ambipolar diffusion equation is charge neutrality. Since the electron diffusion constant is higher than the hole diffusion constant, the charge will attempt to separate. Consequently, a field $E_i$ is produced

in the opposing direction to prevent further separation.[12] This equilibrium is described by

$$E_i = \frac{kT}{q} \frac{b-1}{nb+p} \nabla \delta p \tag{10}$$

This is simplified to

$$E_i = - \frac{kT}{q} \frac{b - 1}{b + 1 + b \frac{n_i}{\delta p}} \frac{r}{2Dt} \tag{11a}$$

or,

$$E_i = - \frac{kT}{q} \frac{1}{3+2n_i/\delta p} \frac{r}{2Dt} \quad b \simeq 2 \tag{11b}$$

Figure 4 shows this function. The behavior is in good agreement with profiles produced by a Computer Code solution.[4]

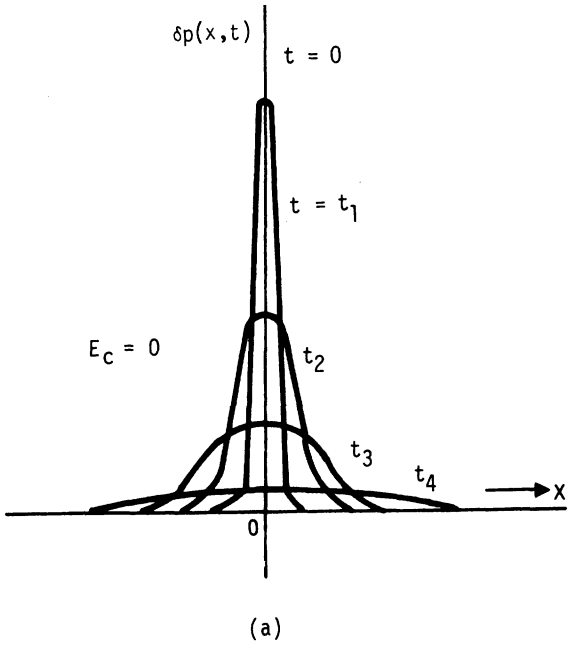


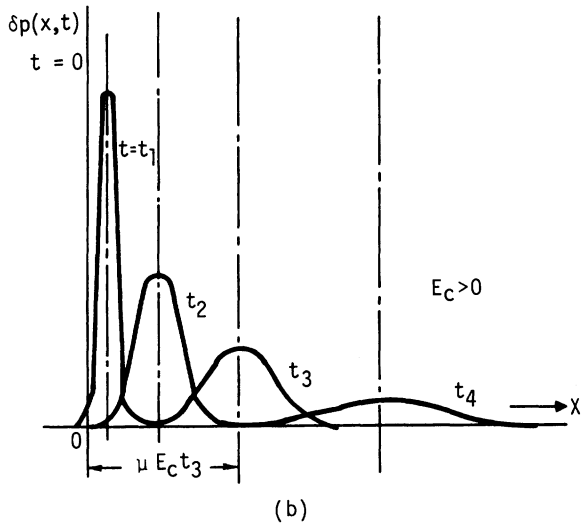


Figure 4. Carrier Concentration vs Time

The excess carriers created along the ion track must decay due to recombination in the absence of any external field or current. This is verified as follows,

$$\int_0^\infty \int_0^{2\pi} \delta p(r,\theta,t) r dr d\theta = N \exp\left(-\frac{t}{\tau}\right) \tag{12}$$

A detailed examination of eq (9) and Figure 3 shows that even in the presence of a field, the initial motion is entirely due to diffusion. At long times, the carrier motion is entirely due to the field. At any particular time t, the relative importance of drift and diffusion can be assessed by comparing $\sqrt{Dt}$ with $\mu E_c t$ since $\sqrt{Dt}$ is the radial diffusion distance and $\mu E_c t$ is the linear drift distance along the field. For many cases of practical interest, the process can be approximated by considering the carrier motion in two separate stages: first, a radial expansion until $N/4\pi Dt \simeq n_i$, then motion along the electric field.

Again, for many cases of practical interest, field motion starts after the ion track radius has expanded from its initial value of about 0.1 μ to a value of about 1 μ. The track is created in a few picoseconds and the expansion to 1 μ requires about 500 picoseconds. Figure 5 shows a comparison of $r = \sqrt{Dt}$ and $X = \mu E_c t$.

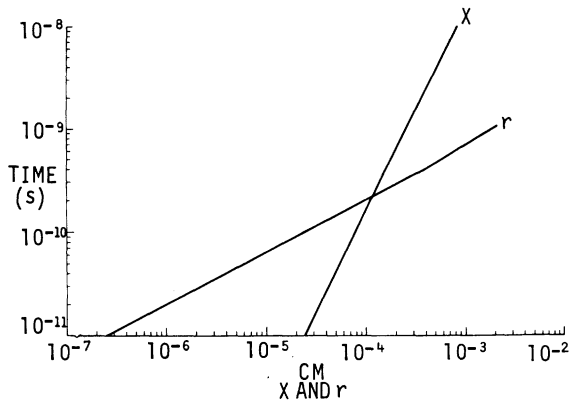


Figure 5. Motion Along Column and Perpendicular to Column

## Ion Tracks Through P-N Junctions

First consider the case where the ion penetrates the junction normally and stops within the junction: Case 1 in Figure 1 with θ = 0 and the track length ℓ equal to or less than the junction width, xj. The carrier motion is governed by eq (3) and (4) which simplify to

$$\frac{d\delta p}{dt} = - \frac{1}{q} \nabla \cdot Jp - \frac{\delta p}{\tau} \tag{13}$$

A specific density of hole electron pairs is assumed initially at $t = t_o \simeq 1/\beta$ with the subsequent generation rate Gp = 0. The initial carrier motion will be radial governed by ambipolar

diffusion. However, when the carrier concentrations become comparable to the doping concentration in the junction, the junction field asserts itself and current flow along the junction field occurs. At this time, diffusion parallel to the track is negligible, $-qD_p\nabla P \simeq 0$, and

$$\frac{d\delta P}{dt} = -\mu_p \delta p \frac{dE}{dX} - \frac{\delta p}{\tau} \tag{14}$$

Integrating,

$$\delta P = \frac{N}{4\pi Dt} \exp\left(-\mu_p \frac{dE}{dX} t - \frac{t}{\tau}\right) \qquad t - t_o > t_o \tag{15}$$

where $N/4\pi Dt$ is the hole density in the track. Assuming that the initial track is created by a process involving a simple time constant for thermalizing the hot electrons,

$$\delta p = \frac{N}{4\pi Dt} \left[\exp\left(-\mu_p \frac{dE}{dX} t\right) - \exp\left(-\beta t\right)\right] \tag{16}$$

Here $\tau$ is assumed long compared with times of interest.

For a one-dimensional abrupt junction, $dE/dX = -qN_D/k\epsilon_o$, and $E_o = \sqrt{2qN_D(-V+\phi_o)/k\epsilon_o}$.

Utilizing eq (3) again and noting that area over which the current flows in $4\pi Dt$,

$$I_p = -q\mu_p NE_o\left[\exp\left(-\mu_p \frac{dE}{dX} t\right) - \exp\left(-\beta t\right)\right] \tag{17}$$

The electron current can now be obtained in a similar fashion and,

$$\begin{aligned} 2I(t) = &-q\mu_p NE_o \left[\exp\left(-\mu_p \frac{dE}{dX} t\right) - \exp\left(-\beta t\right)\right] \\ &-q\mu_n NE_o \left[\exp\left(-\mu_n \frac{dE}{dX} t\right) - \exp\left(-\beta t\right)\right] \end{aligned} \tag{18}$$

This can be approximated by

$$I(t) = -q\bar{\mu}NE_o \left[\exp\left(-\bar{\mu} \frac{dE}{dX} t\right) - \exp\left(-\beta t\right)\right] \tag{19}$$

where

$$\bar{\mu} \simeq \frac{\mu_n + \mu_p}{2} F(E)$$

At this point, the opportunity is taken to correct the mobility for high field effects in the junction using F(E); Appendix A. The time constant for the collection process is the junction time constant $1/\bar{\mu}\frac{dE}{dX}$ or $k\epsilon_o/q\bar{\mu}N_D$.

The total charge collected can be obtained by integrating eq (18) over time from 0 to $\infty$. This gives

$$\int_0^\infty I(t) = -qNX \tag{20}$$

where X is either $X_j$ or $\ell$ depending on whether the track extends to $X_j$ or stops in the junction.

This is exactly the result to be expected since all of the charge created in the ion path will be collected. (Remember recombination was neglected.) This result does, however, provide a good check on the validity of eq (18).

If the ion comes in at an angle $\theta$, the derivation is easily extended,

$$I(t) = -q\bar{\mu}NE_o \sec\theta \left[\exp\left(-\bar{\mu} \frac{dE}{dX} t\right) - \exp\left(-\beta t\right)\right] \tag{21}$$

Remember that $NX\sec\theta$ must always be limited to less than $N\ell$, the total charge in the track, or $NX_j \sec\theta$ if the track extends to the edge of the junction.

The use of a constant mobility in eq (14) is justified by the approximation involving separating the radial diffusion and the collection along the direction of the junction field into two sequential stages: radial ambipolar diffusion followed by collection in the direction of the field with normal mobilities. Another approximation is possible by integrating eq (14) with a time-dependent transitional mobility function. For this purpose, assume the time dependence from Appendix A. Thus,

$$\begin{aligned} I(t) = -q\bar{\mu} \frac{t}{t_o} NE_o \sec\theta \left[\exp\left(-\bar{\mu} \frac{dE}{dX} \frac{t^2}{2t_o}\right)\right. \\ \left. - \exp\left(-\beta t\right)\right] \quad t < t_o \end{aligned} \tag{22}$$

For $t > t_o$ use eq (21). (The amplitude will have to be adjusted to the value from eq (21) at $t = t_o$.)

It is expected that eq (21) will prove to be a simple and adequate approximation and that the additional complexity of eq (22) will not provide a really worthwhile refinement. However, the t square dependence in eq (22) is apparent in the model results from Hsieh's[1] computer code results, and the fit suggested by Hu[3].

## The Funnel Phenomenon

When the ion penetrates through the junction and into the substrate, charge can be rapidly collected from a portion of the track in the substrate. This was not anticipated in the early models which assumed that the charge would have to diffuse from the substrate to the edges of the junction and then be collected by the junction field.[2]

The funnel phenomenon is easily explained by realizing that the radius of the ion track is extremely small and thus a large spreading resistance is created from the edge of the junction into the substrate. The IR drop created is in the direction to cause field enhanced collection of charge from a portion of the track in the substrate. The original voltage across the junction is redistributed so that part of it appears across the junction and the rest of it across the substrate. This is shown in Figure 6. The field decreases directly proportional to distance in the junction when the charge is being collected, due to the one-dimensional nature of the junction. However, the field falls off quadratically in the substrate due to the two-dimensional nature of substrate current flow. A good first approximation to the length of the funnel is obtained by extrapolating the linear drop in the junction until the field reaches 0.

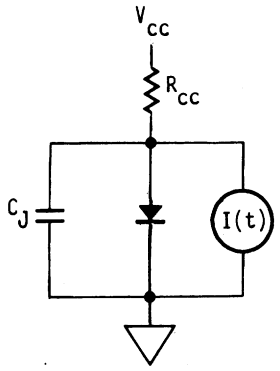


(a) Simple Equivalent Circuit

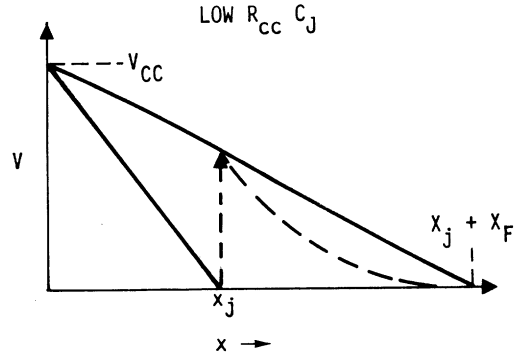


(b) Funnel Formation Using Linear Approximation

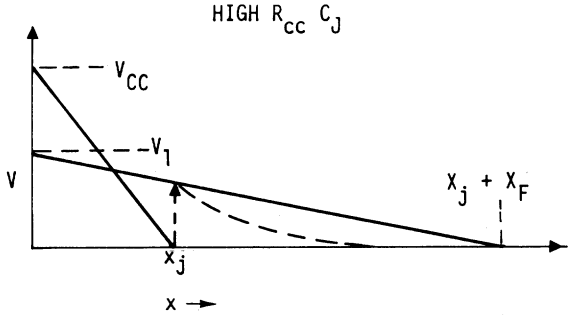


(c) Funnel Formation Using Linear Approximation

$R_{CC} C_J < 10^{-10}$ s NO CHANGE OF LOGIC STATE

$R_{CC} C_J > 10^{-9}$ s LOGIC STATE MAY CHANGE

(ASSUMES Q $C_J$ > 3 V)

Figure 6. Circuit Effects

The current I(t) builds up to a maximum at approximately the time $\delta p = N_D$ and the transition between ambipolar radial diffusion and field driven collection is occurring. It is approximately at this time that the field caused by the IR drop in the substrate produces the maximum funnel length. The following "first cut" approximations are suggested to estimate I(t) when funneling is significant. The time $t_1$ at which $\delta p = N_D$ is obtained from eq (8),

$$t_1 = \frac{N}{4\pi D_p N_D} \tag{23}$$

The effective radius of the spreading resistance is approximated as $\sqrt{D_p t_1}$ and the spreading resistance is approximated by $R_s = \rho/4\sqrt{D_p t_1}$; Appendix B, where $\rho$ is substrate resistivity. This neglects the effect of the lower resistance applicable to the portion of the track in the substrate. This approximation is valid since the IR drop at early times is dominated by the portion of the track in the junction. The substrate drop, IRs, is estimated using eq (21) as $V_S = q\bar{\mu}NE_o R_s$. Next, eq (21) is modified to include the funnel.

$$I(t) = -q\mu NE_o \sec\theta \left(\frac{V_o}{V_o - IRs}\right) [\exp(-\bar{\mu}\frac{dE}{dX} t) - \exp(-\beta t)] \tag{24}$$

For practical limitations $\frac{V_o}{V_o - IRs}$ must be less than 5, and $\frac{V_o}{V_o - IRs}$ NXsec$\theta$ must be less than N$\ell$ the total charge in the track.

This approach should give good results for funnels comparable in length to the junction width, but the approximation is expected to get worse for long funnels. This is because both diffusion and field collection overlap significantly for long funnels.

Figure 2 shows calculated currents from 5 MeV $\alpha$ tracks for two typical junction doping levels. The parameters were picked to facilitate comparison with the Hsieh[1] computer model results. The comparison shows good agreement in both time constant and amplitude. However, the low doped substrate has a higher value of peak current than the higher doped substrate which is inconsistent with the Hsieh computer model. The relatively good agreement in amplitude is considered fortuitous because of the many assumptions involved in estimating the funnel parameters. However, the agreement in time constant is more significant since only a few assumptions are necessary in deriving the time constant. The agreement in amplitude is much better for the higher doped case, and for both cases these calculations result in higher values of current than the computer model. The computer model accounts for variation of LET along the track, whereas this calculation assumes a constant value of $4 \times 10^8$/cm. This may account for most of the discrepancy.

Detailed comparison of eq (24) with experimental data is planned. For modeling purposes, the best fit will be obtained by inserting two adjustable constants. $t_1$ in eq (23) will be regarded as $\alpha t_1$ and the best value of $\alpha$ determined by comparison to data. The determination of $R_s$ will be regarded as $\beta R_s$ and the best value of $\beta$ determined by comparison to data.

The junction time constant in eq (24) is a slowly increasing function of funnel length. When the applied voltage readjusts so that part is dropped across the junction and part across the spreading resistance, dE/dX obviously decreases in proportion to the total distance (junction width plus funnel length) over which field collection occurs. However, a partially compensating increase in mobility, $\bar{\mu}$, occurs because of the lower average field. That is, F(E) increases toward unity in eq (19).

## Circuit Effects

The effect of a cosmic ray event on an integrated circuit can be determined by introducing the time dependent current generator into the equivalent circuit in exactly the same way as photocurrent generators have been accomodated. The simplest case is illustrated in Figure 6. The current generator must be inserted directly across the junction as is done in the SYSCAP code; it cannot be inserted from Vcc to ground as is sometimes done for photocurrent generators in other computer codes.

The most obvious circuit effect is also illustrated in Figure 6. When $RccC_J$ is small compared with time constant for charge collection from the ion path, Vcc controls the junction voltage and upset or logic state change cannot occur (Figure 6b). When $RccC_J$ is long compared with the charge collection time constant, the junction voltage is controlled by the charge collected from the ion track (Figure 6c). In this case, for 5 volt logic, if the capacitance times the charge collected exceeds about 3 V, the node will discharge to Vl and logic upset or change of state will occur.

In any case, the insertion of the time-dependent current generator into the equivalent circuit will faithfully predict the transients or change of status produced in the IC by the ion track event.

It is obvious that the parameters of the equivalent circuit can affect the circuit consequences of ion tracks in a major way.

## Summary

Charge motion resulting from the passage of a high energy ion through semiconductors and semiconductor devices has been determined. In a homogeneous semiconductor, radial ambipolar diffusion occurs and a closed form analytical solution is derived to summarize the charge relaxation process back to an equilibrium condition. The effect of a constant perturbing field in the X direction is also analytically determined in a closed form expression.

The analysis is extended to include the case when the ion passes through an abrupt n-p junction and then into a homogeneous substrate. The junction collects the charge created by the ion with a time constant approximately equal to the junction time constant, $k\epsilon_o/q\mu N_D$. This is most readily explained by separating the charge motion into two sequential steps: (1) radial ambipolar diffusion until the excess charge density is approximately equal to the background doping density and (2) charge collection on the junction node driven by the junction field. An approximate closed form solution for the junction current, I(t), is derived which reveals the important design variables to minimize the transient upset or soft error problem in ICs.

An important effect called funneling can result when the ion track extends into the substrate. The IR drop produced in the substrate when the charge collection process occurs extends the junction field into the substrate in a direction to enhance the charge collection process. An approximate procedure for estimating the IR drop in the substrate and the length of the funnel is described. This leads to an approximate closed form expression for the collected current I(t) including the funnel effect.

From a modeling standpoint, the effect of the collected charge from an ion track is described by inserting the current generator I(t) across the sensitive junction or junctions in an IC using a computer code program such as SYSCAP. This process allows for all of the complex current interactions in the IC to take place and provides a mechanism for evaluating the effects of all of the design variables inherent in the charge collection process on the soft upset problem.

## References

1. C. M. Hsieh et al, "Dynamics of Charge Collection from α-Particle Tracks in Integrated Circuits," Proc. IEEE International Reliability Physics Symposium, pp. 38-42, Orlando, Florida, April 7, 1981.

2. S. Kirkpatrick, "Modeling Diffusion and Collection of Charge from Ionizing Radiation in Silicon Devices," IEEE Transaction on E.D., ED-21, No. 11, November 1979, pp. 1742-1753.

3. C. Hu, "α-Particle-Induced Field and Enhanced Collection of Carriers," IEEE E.D. Letters, Vol. EDL-3, #2, February 1982, pp. 31-34.

4. H. Gruben, Private Communication.

5. J. Bradford "Nonequilibrium Radiation Effects in VLSI" IEEE Trans. Vol. NS-25. No. 5, Oct. 1978, pp. 1144.

6. W. Heinrich, "Calculation of LET-SPECTRA of Heavy Cosmic Ray Nuclei at Various Absorbtion Depths," Radiation Effects, Vol. 34, pp. 143-148.

7. G. Jaffe, ANNALEN der PHYSIK, 42, 1913, 303.

8. C. Powell, "The Nature of Primary Cosmic Radiation," Proc. 11th International Conference on Cosmic Rays, Budapest, 1969, pp. 9.

9. Runyan, "Silicon Semiconductor Technology," McGraw-Hill, 1965.

10. Torrey & Whitmer, "Crystal Rectifiers," Radiation Lab Series, McGraw-Hill, 1948.

11. McKelvey, "Solid-State and Semiconductor Physics," Harper and Row, 1966.

12. Von Roos "A Note on Photocurrents in Extrinsic Semiconductors" Solid State Electronics 1979 Vol. 22 pp. 229-232.

## Appendix A. Transition Functions

The ambipolar equation and the regular diffusion equation are identical except for the values of diffusion constant and mobility. At early times, carrier motion is ambipolar and the ambipolar diffusion constant D* governs carrier motion. At long times the regular diffusion constants either Dp or Dn govern carrier motion. The continuity equation can be solved in closed form for a constant value of D; D* early in time or Dp/Dn late in time. The diffusion Constant D is concentration dependent. The correct transition from ambipolar diffusion constant to normal diffusion constant is given by [11]

$$D = (n_i + 2\delta p)\, DnDp/[(n_i + \delta p)\, Dn + \delta p Dp] \qquad (A\text{-}1)$$

For very high values of $\delta p$,

$$D = D^* = 2DnDp/(Dn + Dp) \qquad (A\text{-}2)$$

where $n_i \simeq N_p$ the background concentration in

the silicon material. For very low values of $\delta p$, D = Dp. In the same way a transition function for mobility is obtained:

$$\mu = \frac{(\delta p + n_i - \delta p)\,\mu_n\mu_p}{(\delta p + n_i)\mu_n + \delta p\mu_p} = \frac{n_i\,\mu_n\mu_p}{(\delta p + n_i)\mu_n + \delta p\mu_p} \qquad \text{(A-3)}$$

At very high values of $\delta p$,

$$\mu = \mu^* = \frac{n_i}{\delta p} \cdot \frac{\mu_n\mu_p}{\mu_n + \mu_p} \simeq 0 \qquad \text{(A-4)}$$

And at very low values of $\delta p$, $\mu = \mu_p$

The value of D changes from approximately 18 to 13 in lightly doped n-type silicon substrates. Thus, eq (8) with D given by eq (A-2) is a very good approximation. However, the value of $\mu$ changes from approximately 0 to 500 in a lightly doped n-type silicon substrate. Thus, eq (9) with $\mu$ given by eq (A-3) could produce significant errors. Looking at the asymptotic exact solutions, it is estimated that the error is banded by $\delta p \pm 0.50\,\delta p$ with the maximum error occurring at $\delta p = n_i$.

For purposes of obtaining a better approximation to the junction time constant, the value of $\mu$ is assumed to increase linearly with time. Thus,

$$\mu = \mu_o t/t_o \qquad 0 < t < t_o$$
$$\mu = \mu_o \qquad t > t_o \qquad \text{(A-5)}$$

Mobility generally becomes dependent on the applied field at large values of field. This dependence has been carefully measured[9] and is shown in Figure A-1. Figure A-1(a) shows the transition from ambipolar mobility to $\mu_n$ or $\mu_p$ in bulk. Figure A-1(b) shows the transition from ambipolar mobility to $\mu F(E)$, the reduced mobility in a high field of value E. This transition is assumed linear with time in obtaining eq (22).

When charge collection occurs from a funnel, the average value of E drops and the average value of mobility increases. Thus, the product $\mu E$ will decrease proportional to the square root of the total path length involved in the charge collection process. The approximate treatment for short funnels assumes $\mu E$ is constant. For long funnels a correction may be necessary.

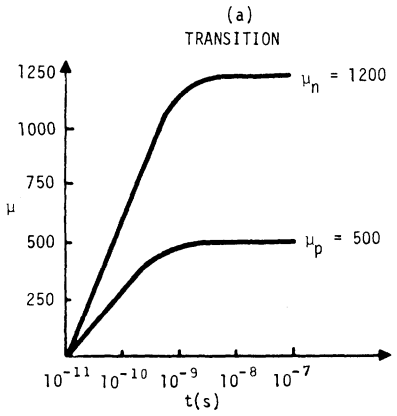


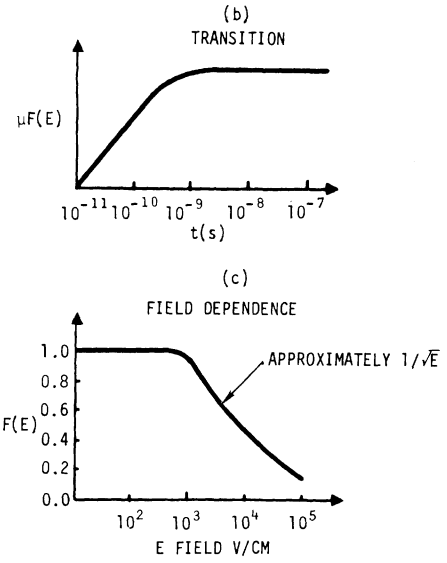


Figure A-1. Mobility Considerations

## Appendix B. Substrate Spreading Resistance

When an ion penetrates a junction and the substrate region below the junction, the cross-section of the column at the junction substrate interface is circular for normal incidence and elliptical for incidence at an angle $\theta$. The ellipse will have minor radius a and major radius a $\sec\theta$. However, before any significant charge collection can occur, the ambipolar diffusion of the charge collection in the radial direction will produce an approximately circular interface.

This interface is the neck of the spreading resistance. Spreading resistance from an elliptical constant into a uniformly charged substrate is given by[10]

$$R_S = \frac{K}{2\pi\sigma a \sec\theta} \qquad \text{(B-1)}$$

where $K = sn^{-1}(1,k)$ and $k = \sin\theta$. Equipotential surfaces in the substrate are confocal ellipsoids, and field lines are hypoerboloids of revolution. (Figure B-1).

The circular interface case gives $R_S = \frac{1}{4\sigma a}$. This is a good approximation for all except the largest values of incident angle $\theta$. Figure B-2 shows the Field and Equipotential surfaces for a normal ion track through a p-n junction.

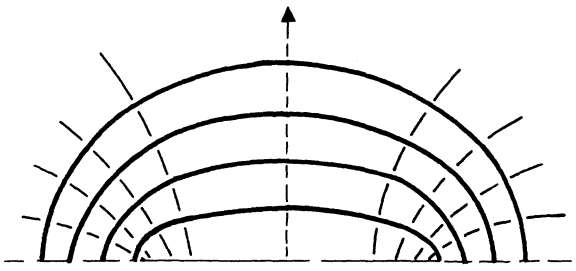

Figure B-1. Section Through a Circular Contact Showing the One Sheet Hyperboloids Which Define the Field and the Orthogonal Oblate Speriods Which Define the Equipotential Surfaces

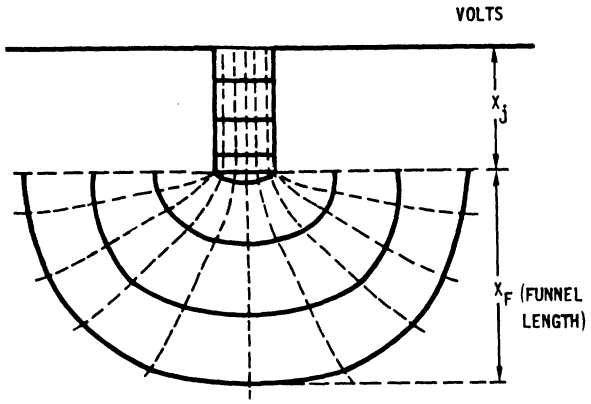


$$R_S = \frac{1}{4a\sigma} \qquad \text{CIRCULAR CONTACT}$$

$$R_S = \frac{K}{2n\sigma a} \qquad \text{ELLIPTICAL CONTACT}$$

K COMPLETE ELLIPTIC INTEGRAL FIRST KIND

MODULUS $k = (1 - b^2/a^2)^{1/2} = \sin\theta$

$$\frac{X_F + X_j}{X_j} = \frac{V}{V - I_M(t)\, R_S}$$

Figure B-2. Potential and Field Lines for a Normal Ion Track Through a P-N Junction

Acknowledgment

This research was primarily funded by Autonetics Strategic Systems Division. In addition, significant funding was provided by Litton Corporation and by the Defense Nuclear Agency.

Helpful suggestions were received from Dr. Oldwig Von Roos, Dr. John Zoutendyk, and Dr. Loren McMurray. Their contributions are gratefully acknowledged.